

PAUL SCHERRER INSTITUT



Chavdar Dutsov :: Paul Scherrer Institute

# Systematic effects in the search for the muon EDM using the frozen-spin method

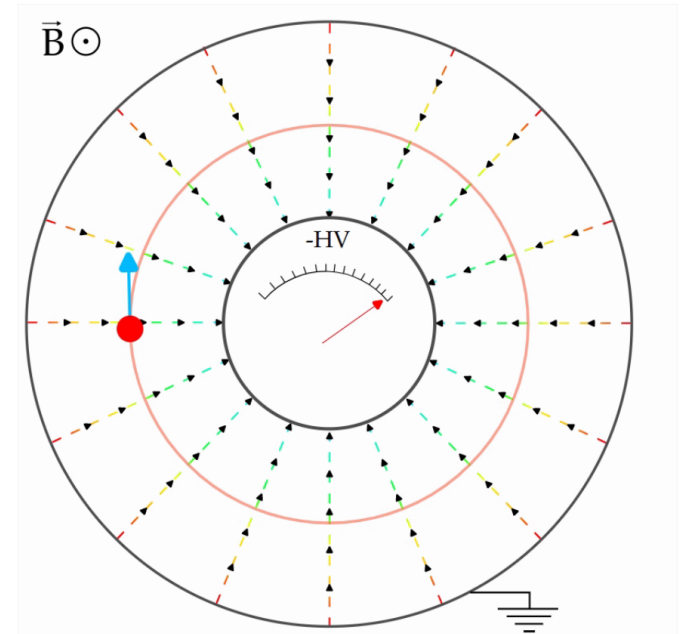
On behalf of the muonEDM collaboration

16 May 2023 – Pisa

# Frozen spin technique in a nutshell

- Relativistic spin precession of a charged particle (Thomas-BMT equation) →
- By applying an appropriate radial E-field to the muon we negate the  $g-2$  term.
- Ideally any observed spin precession would be due to a non-zero EDM.
- Asymmetry between upstream and downstream emitted decay positrons.
- **Some asymmetry could still be observed due to systematic effects**

$$\vec{\Omega} = -\frac{e}{m_0} \left[ \underbrace{a\vec{B} + \left( \frac{1}{\gamma^2 - 1} - a \right) \frac{\vec{\beta} \times \vec{E}}{c}}_{g-2 \text{ term}} + \underbrace{\frac{\eta}{2} \left( \frac{\vec{E}}{c} + \vec{\beta} \times \vec{B} \right)}_{\text{EDM term}} \right]$$



# Systematic effects

- Effects that lead to a *real* or *apparent* precession of the spin around the radial axis that are not related to the EDM.
- Types of systematic effects:
  - Early to late variation of detection efficiency of the EDM detectors (*apparent*)
  - Coupling of the anomalous magnetic moment with the EM fields of the experimental setup (*real*)

- Dynamical phase

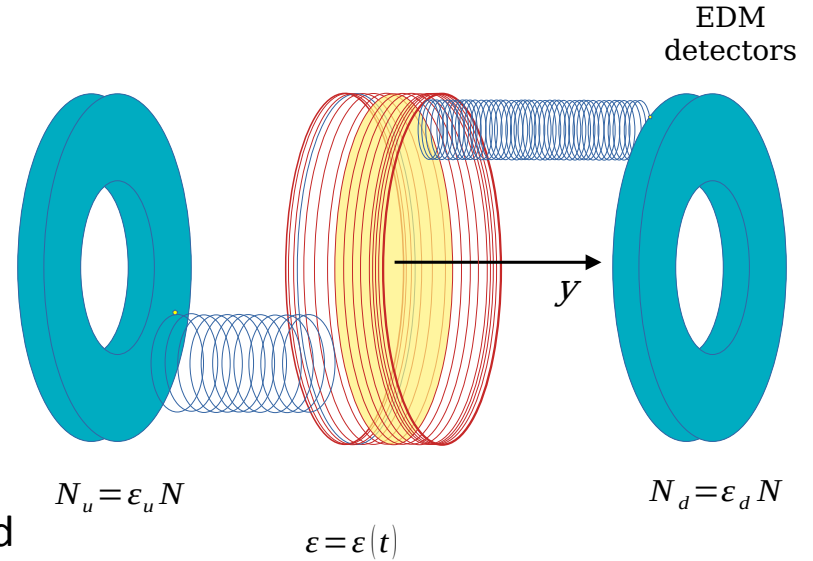
$$\vec{\Omega}_{\text{MDM}} = -\frac{e}{m_0} \left[ a\vec{B} - a\frac{\gamma-1}{\gamma} \frac{(\vec{\beta} \cdot \vec{B})\vec{\beta}}{\beta^2} + \left( \frac{1}{\gamma^2-1} - a \right) \frac{\vec{\beta} \times \vec{E}}{c} \right]$$

- Geometric phase

$$\gamma_n[C] = i \oint_C \langle n, t | (\nabla_R |n, t\rangle) dR$$

# Early-to-late detection efficiency changes

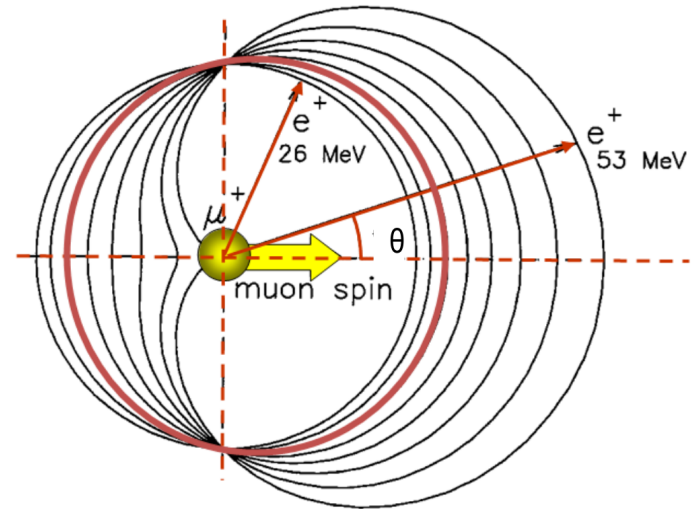
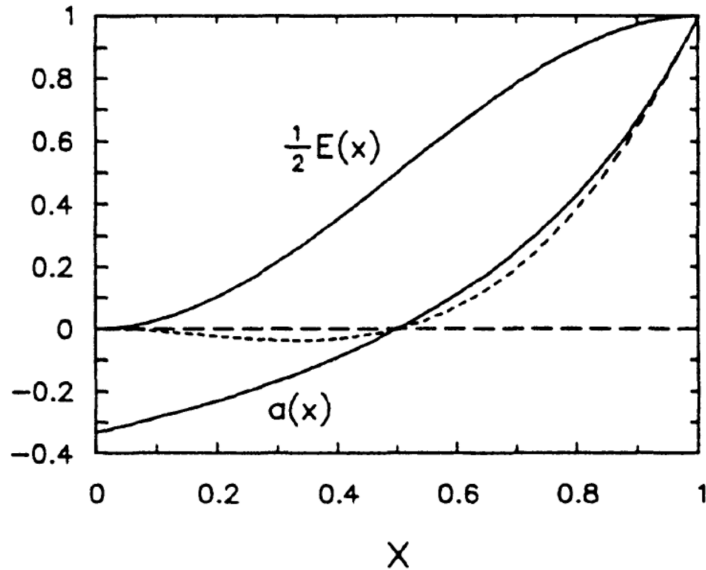
- Strong pulsed magnetic field  $\rightarrow$  eddy currents, noise, heat in detectors and associated electronics.
- **Time-dependent changes in the detection efficiency of a set of detectors will be seen as a false EDM signal.**
- Significant only for low-energy positrons that would produce a weak signal and could be missed by the detectors.



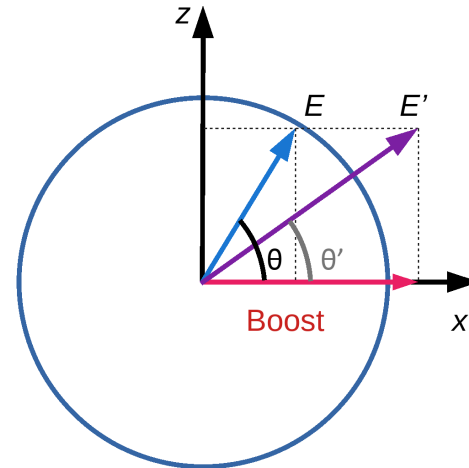
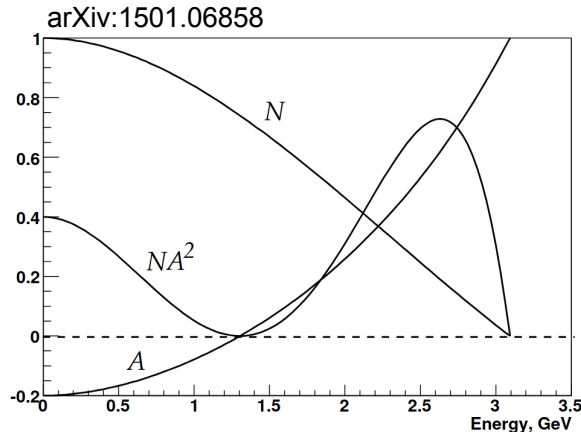


# Kinematics of Michel decay positrons

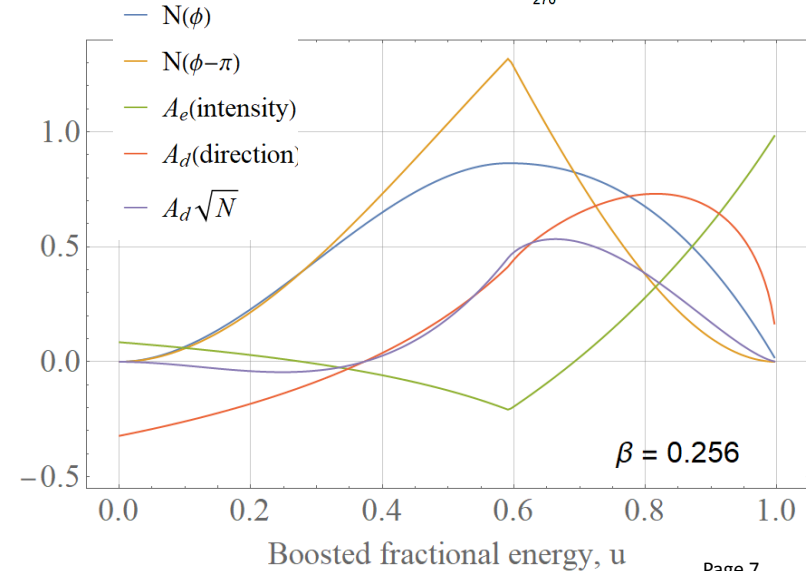
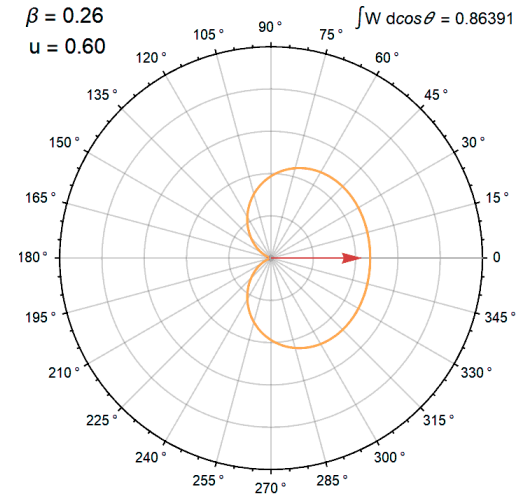
- For high positron energies – preferentially emitted in the direction of the muon spin.
- Energy spectrum and **directional** asymmetry as a function of the fractional energy  $x = E/E_{max}$ :



- For high momentum muons the angular distribution is Lorentz boosted along the momentum.
- For large boosts practically all decay positrons are emitted in the forward direction – **no directional asymmetry**.
- **Intensity asymmetry:** Dependence of the number of decay positrons at a given energy on the spin.



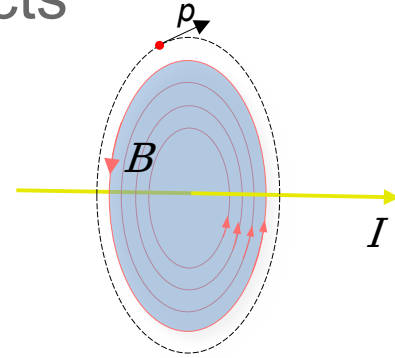
- The first stage – 28 MeV/c surface muons.
- Both **directional** and **intensity** dependence on the spin direction.
- Precession due to the g-2 can be measured using intensity asymmetry.
- Precession due to EDM can be measured from the direction of emitted positrons:
  - up-down asymmetry.
- Only positrons above 25 MeV contribute significantly to the asymmetry.



# Real spin precession systematic effects

- Only four sources of spin precession that could lead to EDM-like signal:
- Net azimuthal B-field  
(zero if no current flows through the area enclosed by the orbit)
- Time variable radial B-field  
(constraints on the pulse width and decay time of the magnetic kick)
- Net longitudinal E-field
- Geometric phases

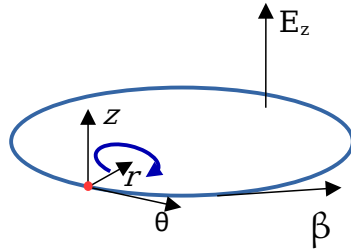
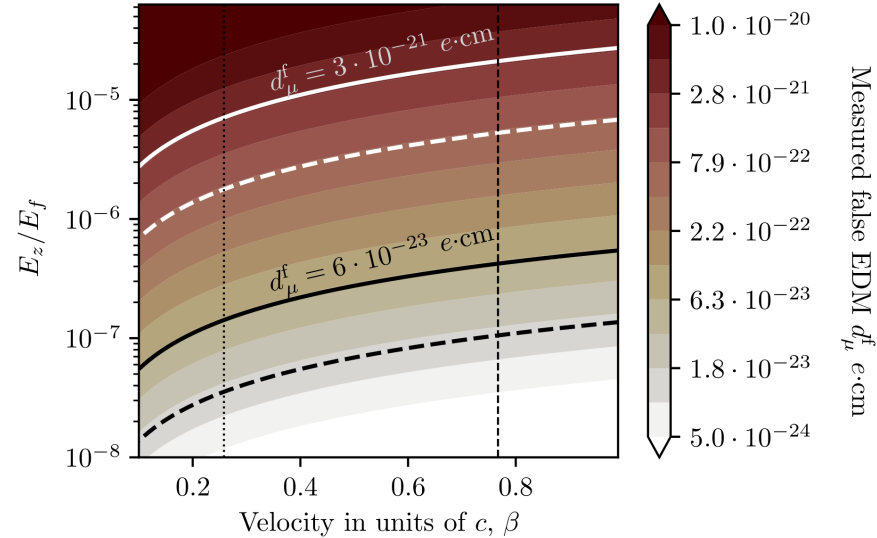
$$\langle (\vec{\Omega}_{\text{MDM}})_\theta \rangle = -\frac{e}{m} \langle B_\theta(t) \rangle$$



$$\langle (\vec{\Omega}_{\text{MDM}})_\rho \rangle = -\frac{ea}{mc} \left\langle \left( 1 - \frac{1}{a(\gamma^2 - 1)} - \frac{1}{\beta_\theta^2} \right) \beta_\theta \right\rangle \langle E_z \rangle$$

# Constraints on the average longitudinal E-field

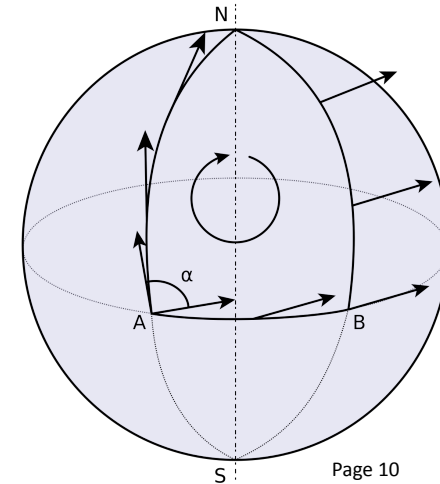
- Limit on the average  $E_z$  field as a function of the muon velocity shown as a fraction of the radial component:
- **Effect cancels if particles are injected alternatively CW and CCW and subtracting counts in the detectors.**
- CW and CCW orbit directions are done by switching the B-field direction.



$$\langle (\tilde{\Omega}_{\text{MDM}})_\rho \rangle = -\frac{ea}{mc} \left\langle \left( 1 - \frac{1}{a(\gamma^2 - 1)} - \frac{1}{\beta_\theta^2} \right) \beta_\theta \right\rangle \langle E_z \rangle$$

# Geometric (Berry's) phase

- The geometric phase is a phase difference acquired over the course of a cycle in parameter space.
- Parallel transport of a vector around a closed loop.
- The angle by which it twists is proportional to the area inside the loop:
  - In classical parallel transport it's equal.
  - In quantum mechanics it's  $-\frac{1}{2}$  (fermions).
- If oscillations around two axes are combined we can observe a phase shift (false EDM)  
**even if the the time average of each oscillation is zero.**



# Calculation of geometric phases

- Spin precesses around axis  $\mathbf{x}$  with amplitude  $C_1$  and frequency  $\Omega_x$ , and around  $\mathbf{y}$  with amplitude  $C_2$  and frequency  $\Omega_y$ . Phase difference between the two  $\beta_0$ .

$$x = C_1 \sin(\Omega_x t), \quad y = C_2 \sin(\Omega_y t + \beta_0)$$

- The movement of the spin encloses an area  $A$  on some abstract surface. The area can be calculated from Green's theorem:

$$A = \frac{1}{2} \int_{t_0}^{t_1} (xy' - yx') dt$$

- The geometric phase as a function time is then:

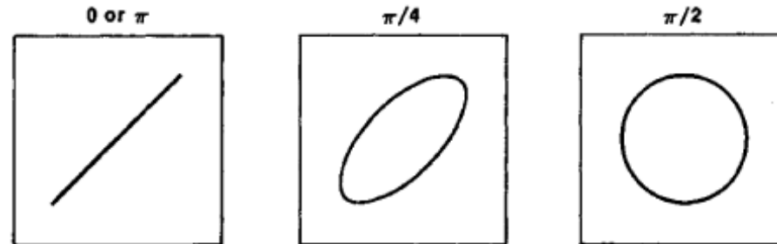
$$\begin{aligned} \alpha(t; \omega_x, \omega_y, \beta_0) &= \frac{1}{2} \frac{\Omega_x \Omega_y}{\omega_x \omega_y} \int (\omega_y \cos(\omega_y t + \beta_0) \sin(\omega_x t) - \omega_x \cos(\omega_x t) \sin(\omega_y t + \beta_0)) dt = \\ &= \frac{1}{4} \frac{\Omega_x \Omega_y}{\omega_x \omega_y} \left[ \frac{\omega_x - \omega_y}{\omega_x + \omega_y} \cos((\omega_x + \omega_y)t + \beta_0) - \frac{\omega_x + \omega_y}{\omega_x - \omega_y} \cos((\omega_y - \omega_x)t + \beta_0) \right] \end{aligned}$$

# Calculation of geometric phases

- In the case where the two oscillations have the same frequency the geometric phase is:

$$\alpha(t; \omega, \beta_0) = \frac{1}{2} \frac{\Omega_x \Omega_y}{\omega^2} \int (\omega \cos(\omega t + \beta_0) \sin(\omega t) - \omega \cos(\omega t) \sin(\omega t + \beta_0)) dt = -\frac{1}{2\omega} \Omega_x \Omega_y t \sin(\beta_0)$$

- The motion of the spin in this case is an ellipse with eccentricity defined by the phase difference between oscillations
  - no phase difference: ellipse looks like a line – no geometric phase
  - $\pi/2$  phase difference: ellipse is a circle and maximum area

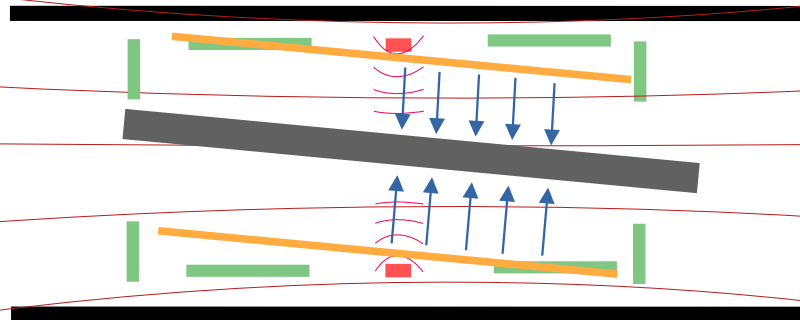
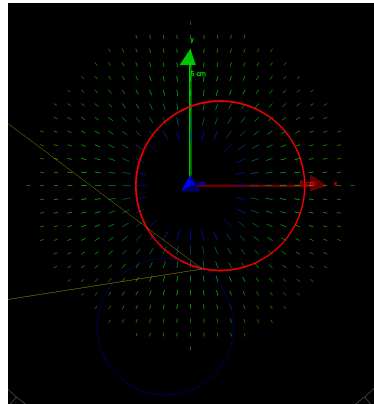




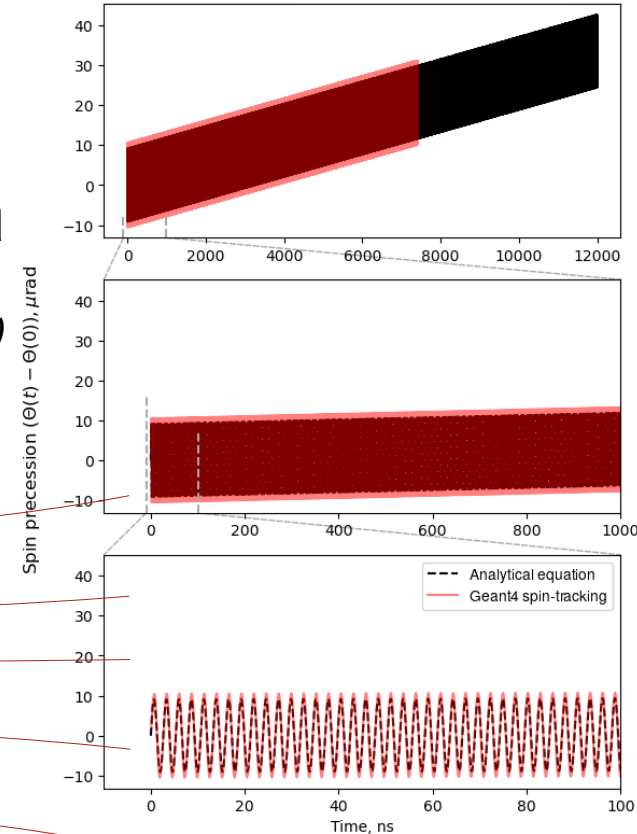
# Example of a geometric phase accumulation

- Spin precession due to misalignment of E-field:
  - longitudinal oscillations due to stronger and weaker freeze field (*cyclotron frequency*)
  - radial oscillations due to longitudinal E-field oscillating between upstream and downstream directions (*cyclotron frequency*)

Tilted and shifted E-field with respect to the center of the muon orbit



$$\alpha(t; \omega, \beta_0) = -\frac{1}{2\omega} \Omega_x \Omega_y t \sin(\beta_0)$$



# Conclusions

- Major sources of possible systematic effects in the experiment are:
- Early-to-late variations in the detection efficiency of the EDM detectors:
  - Only higher energy positrons above 25 MeV contribute to the measured asymmetry.
- Non-zero longitudinal E-field component:
  - Effect cancels if we alternate between CW and CCW injections, determined by the polarity of the main solenoid.
- An analytical description of the geometric phases was developed and tested with G4 simulations:
  - Places constraints on the E-field uniformity and alignment of the injection.

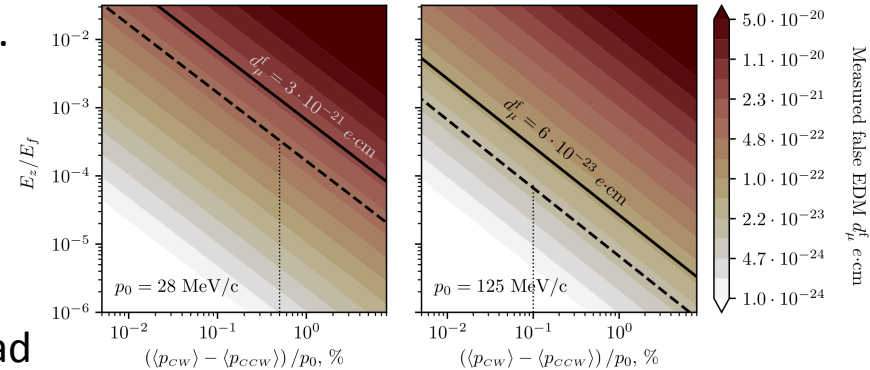
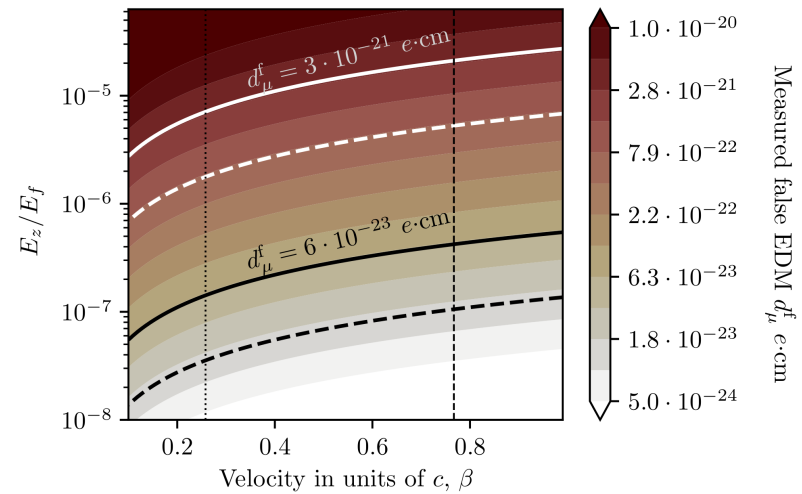
# Thank you for the attention!

muonEDM  
collaboration kick-off  
meeting May 2022  
(Pisa, Italy) →



# Net longitudinal E-field

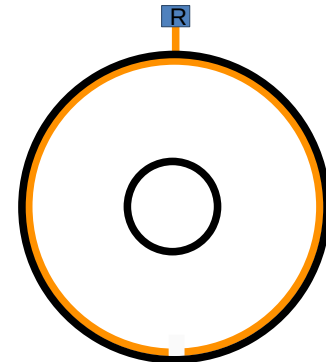
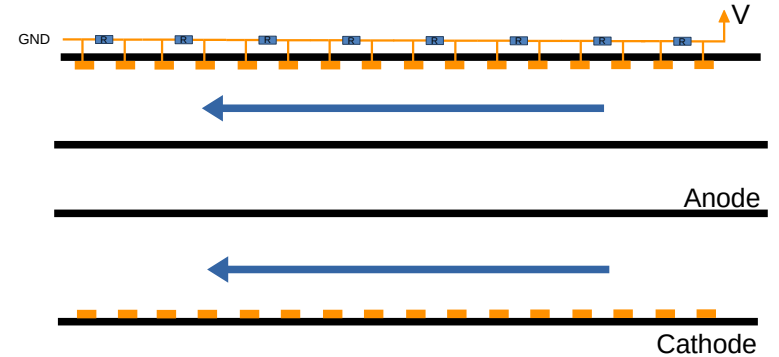
- Very stringent limit on the net longitudinal E-field.
- The effect changes sign with  $\beta$ .  
(change in the longitudinal B-field direction)
- This places limits on the average muon momentum for CW and CCW injections.
- The cancellation works only if:
  - the muon orbits are in the same place for CW/CCW
  - E-field non-uniformity does not lead to too different average  $E_z$  fields for CW/CCW injections.



$$\left\langle \left( \vec{\Omega}_{\text{MDM}} \right)_{\rho} \right\rangle = -\frac{ea}{mc} \left\langle \left( 1 - \frac{1}{a(\gamma^2 - 1)} - \frac{1}{\beta_{\theta}^2} \right) \beta_{\theta} \right\rangle \langle E_z \rangle$$

# Artificial longitudinal E-field

- One can generate a longitudinal E-field with controllable intensity.
- Could be used to verify that we can observe EDM-like signal.
- Could be tuned to cancel the intrinsic average E-field of an imperfect electrode, e.g.:
  - tune field until no signal is seen for CW, then measure CCW.
  - would increase real signal to systematic effect ratio.



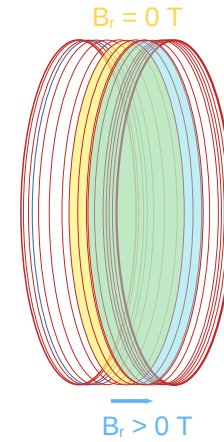
# Limits on real spin precession effects

Systematic effect	Constraints	Phase I		Phase II	
		Expected value	Syst. ( $\times 10^{-21} e\cdot cm$ )	Expected value	Syst. ( $\times 10^{-23} e\cdot cm$ )
Cone shaped electrodes (longitudinal E-field)	Up-down asymmetry in the electrode shape	$\Delta_R < 30 \mu m$	0.75	$\Delta_R < 7 \mu m$	1.5
Electrode local smoothness (longitudinal E-field)	Local longitudinal electrode smoothness	$\delta_R < 3 \mu m$	0.75	$\delta_R < 0.7 \mu m$	1.5
Residual B-field from kick	Decay time of kicker field	$< 50 \text{ ns}$	$< 10^{-2}$	$< 50 \text{ ns}$	0.5
Net current flowing muon orbit area	Wiring of electronics inside the orbit	$< 10 \text{ mA}$	$< 10^{-2}$	$< 10 \text{ mA}$	0.3
Early-to-late detection efficiency change	Shielding and cooling of detectors	–		–	
Resonant geometrical phase accumulation	Misalignment of central axes	Pitch $< 1 \text{ mrad}$ Offset $< 2 \text{ mm}$	$2 \times 10^{-2}$	Pitch $< 1 \text{ mrad}$ Offset $< 2 \text{ mm}$	0.15
TOTAL			1.1		2.2

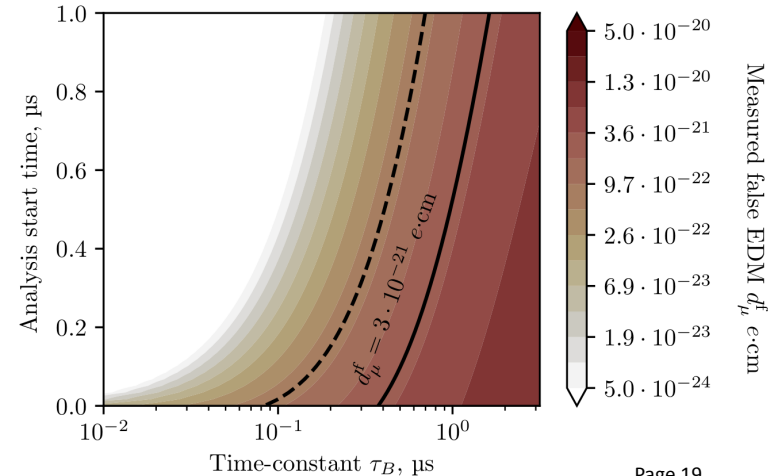
\*assuming electrode shape does not depend on magnetic field orientation

# Time-variable radial B-field

- A static radial B-field would create an offset in the position of the equilibrium orbit.
  - Not a problem since we are interested in the change in the phase with time. \*
- A time-variable  $B_r$  can come from the magnetic kick or eddy currents caused by it.
- Assuming an exponentially decaying residual B-field after the kicker pulse one can determine limits on the decay constant as a function of the analysis start time.
- Radial B-fields of less than 5  $\mu\text{T}$  would not induce a significant spin precession.



$$B_\rho(t) = k B_\rho^{(\text{peak})} e^{-t/\tau_B}$$



\* may or may not induce Berry's phases

# Sources of $E_y$ field: electrode alignment

- The E field of an infinitely long coaxial cylinders is:

$$\vec{E}(\vec{r}) = \frac{V}{\log \frac{b}{a}} \begin{pmatrix} x/r^2 \\ y/r^2 \\ 0 \end{pmatrix}$$

- 

Shifting the field by  $r_0$  and rotating by  $\alpha$  gives:

$$\vec{E}' = R_y(\alpha) \vec{E}(R_y^{-1}(\alpha) \vec{r} + \vec{r}_0) = V_0 \begin{pmatrix} \frac{\xi}{\rho^2} \cos \alpha \\ \frac{v}{\rho^2} \\ -\frac{\xi}{\rho^2} \sin \alpha \end{pmatrix}$$

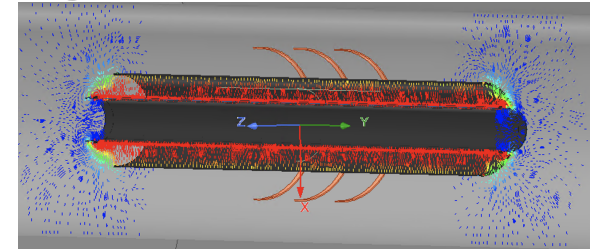
$$V_0 = \frac{V}{\log \frac{b}{a}}, \quad v = y + y_0, \quad \xi = x_0 + x \cos \alpha - z \sin \alpha \quad \text{and} \quad \rho^2 = \xi^2 + v^2$$

- Then average the new field out over a circular orbit:

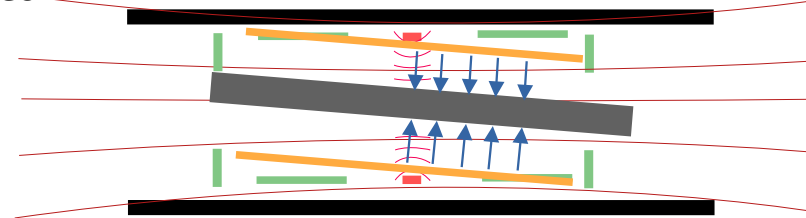
$$\langle E'(\rho, \zeta) \rangle = \frac{1}{2\pi} \int_0^{2\pi} E' d\phi$$

- It can be shown (numerically for now) that:

$$\langle E'(\rho, \zeta) \rangle = \langle E(\rho, \zeta) \rangle$$



Misalignment of the electric field

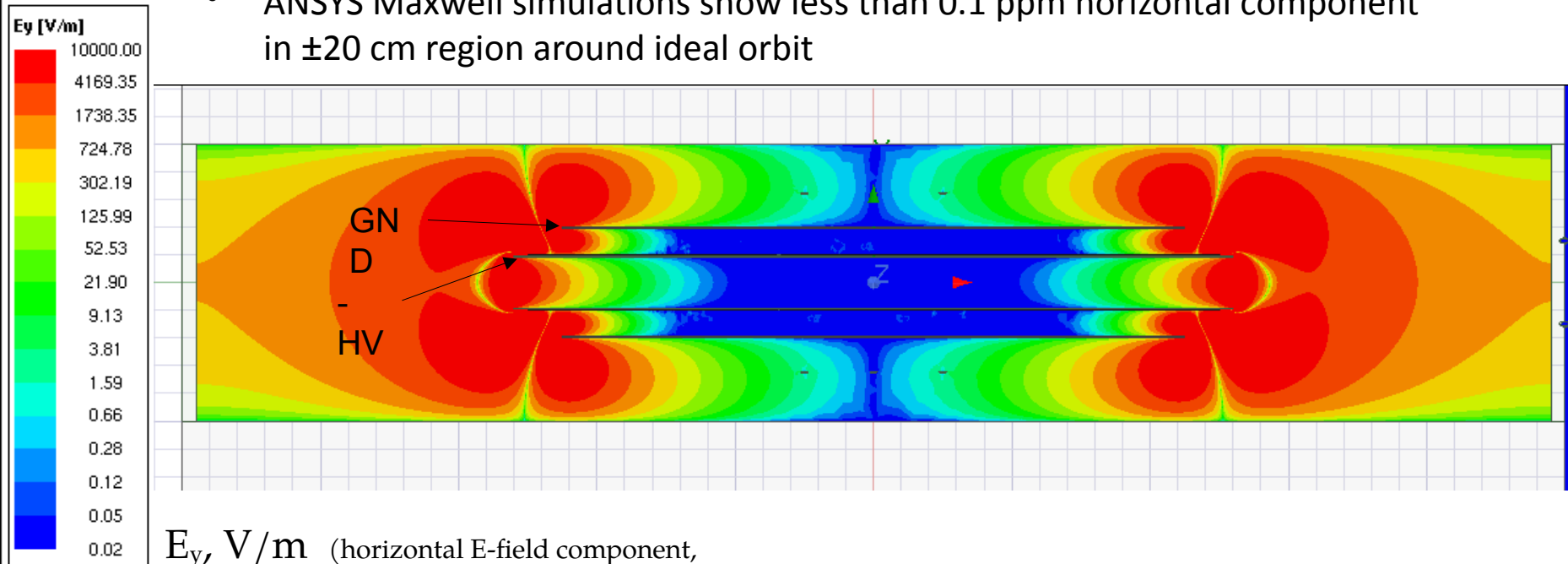


- For a circular orbit the misalignment of the anode or cathode cannot introduce a net horizontal E-field (that was not there before)
- It also does not affect the 'frozen spin' condition



# Sources of $E_y$ field: fringe fields

- The assumption for infinite coaxial cylinders holds if there are negligible fringe field in the region of interest
- ANSYS Maxwell simulations show less than 0.1 ppm horizontal component in  $\pm 20$  cm region around ideal orbit

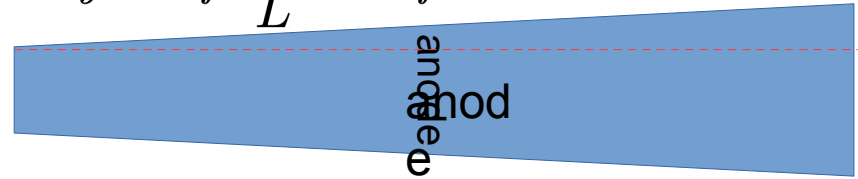


$E_y$ , V/m (horizontal E-field component, logscale)

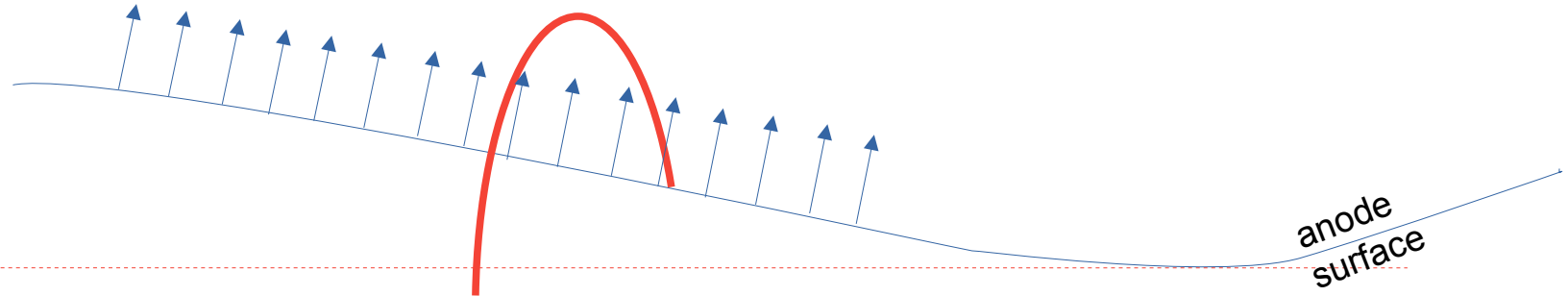
# Sources of $E_y$ field: electrode non-uniformity

- Tapered cone shaped electrodes

$$E_y \approx E_f \frac{\Delta R}{L} \approx E_f \alpha$$



- Smoothness of the electrodes close to the muon orbit (few centimeters)



- Generally sub-micrometer surface smoothness is possible with common machining and polishing techniques
- Cylindricity in the order of 50 nm is measurable even on large samples

# Requirements for electrode uniformity

- The condition to assume ideal uniformity is such that  $E_y$  is kept below the 0.5 ppm from  $E_f$  target
- If the radius of the anode or cathode is larger on one side than on the other then there will be a field component in the vertical direction

- Using a small angle approximation:

$$E_y \approx E_f \frac{\Delta_R}{L} \approx E_f \alpha$$

- The radius of the anode or cathode should not change with more than  $\Delta_R=150$  nm (precursor) and  $\Delta_R=300$  nm (final) along its length ( $L \sim 50$  cm)

# Requirements for electrode uniformity

- Another source of a net vertical field would be a small protrusion on the surface of the electrode
- The E-field of a cylinder with radius  $R$  and surface charge density  $\sigma$  at a distance  $r$  is:

$$E_f(r) = \frac{\sigma R}{\epsilon_0 r}$$

- The E-field from a small protrusion with area  $A$  at a distance  $\Delta_z$  from the storage ring can be calculated from Coulomb's law:

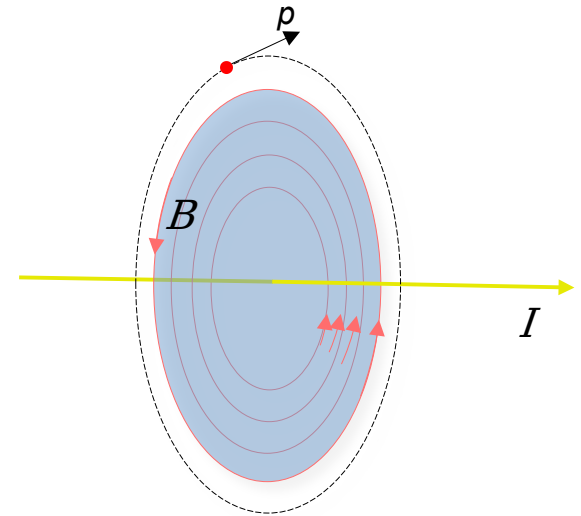
$$E_y(\Delta_z) = \frac{1}{4\pi\epsilon_0} \frac{\sigma A}{\Delta_z^2}$$

- Thus the maximum allowed area for a protrusion is:  $A = 4\pi \frac{\Delta_z^2}{r} \frac{E_y}{E_f}$
- Assuming a spherical cap like protrusion at 2 cm from the storage ring – maximum allowed height  $h = 40 \mu m$

# Limit on the $B$ -field parallel to the momentum

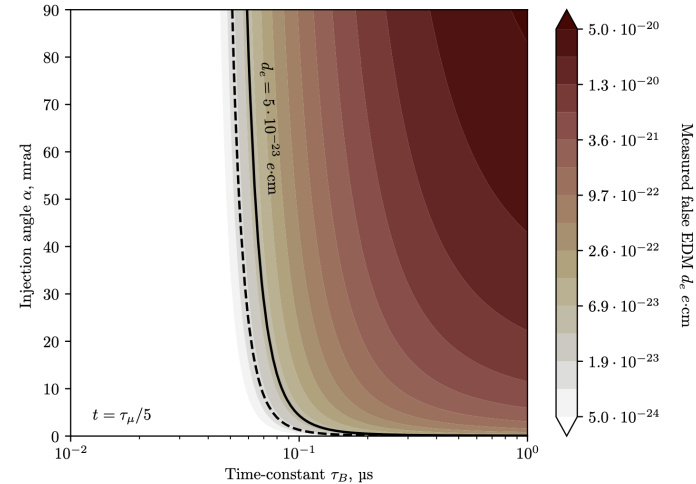
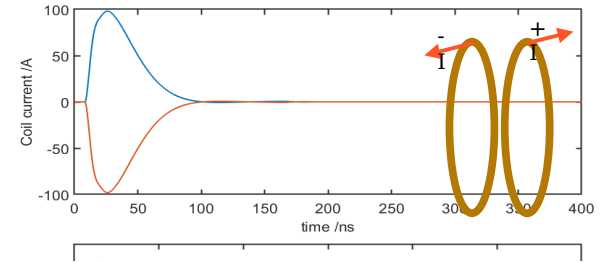
- Non-zero average  $B_z$  field if there is electric current flowing through the area enclosed by the muon orbit
- Write net current!
- From Biot-Savart's law we can give a limit on the systematics due to such current
- Assuming non-insulated wire at the center of the orbit:
  - Precursor:  $I < 250$  mA
  - Final experiment:  $I < 40$  mA

$$\langle \Theta_z \rangle = -\frac{ea}{m_0} \langle B_z \rangle t.$$



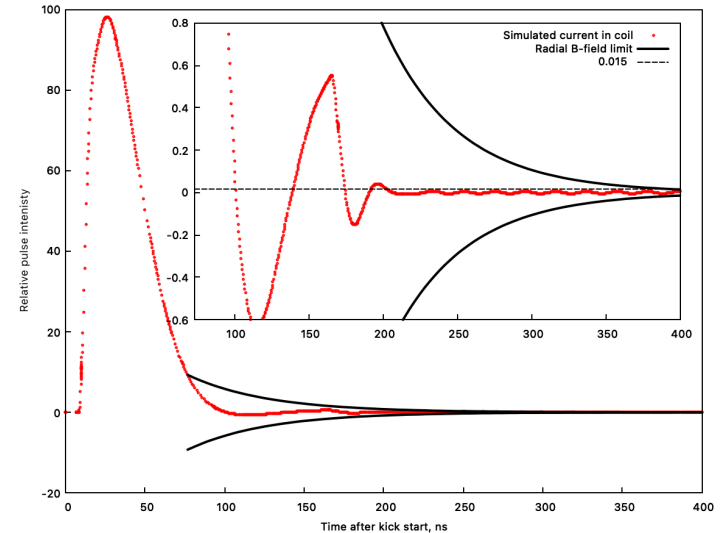
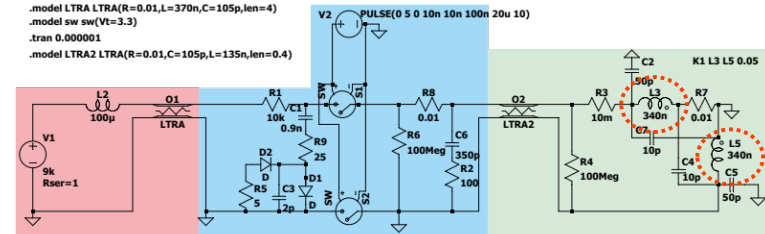
# Limit on the radial $B$ -field

- Limit on the kicker field decay time with relation to the injection angle
- Assumptions:
  - half-sine kicker field intensity
  - end of the kick is considered to be at the 10% from maximum level
  - exponential decay of the ringing signal with time constant  $\tau_B$
  - the limit is such that the influence of the residual field is less than a given  $d_e$  at  $\sim 400$  ns time
- *Note: the constraint is lower for later times and stronger for earlier times*



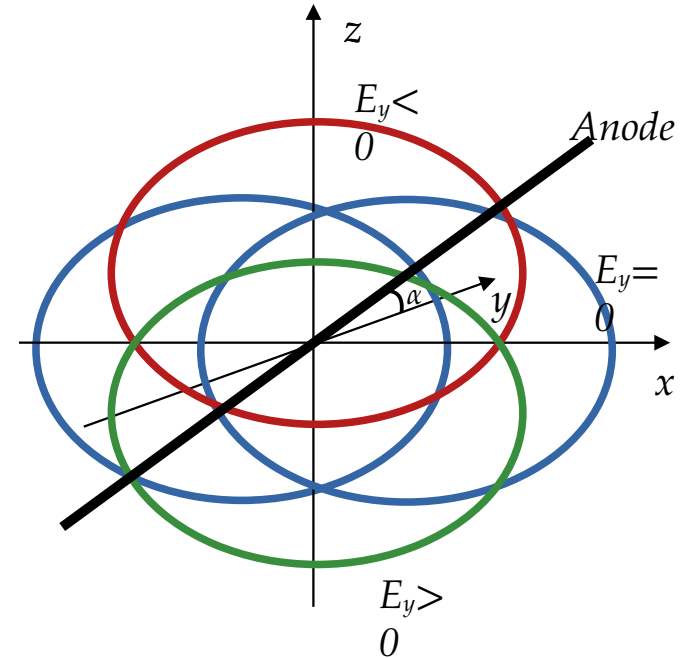
# Limit on the radial $B$ -field

- Simulated short current pulse for the two anti-Helmholtz coils
- The solid black line shows the limiting decay time for an exponentially decaying pulse that goes below the limit at 400 ns (overshoot or undershoot)
- The influence of the simulated kicker field to the observed spin precession is negligible after 200 ns



# Non-circular muon orbit

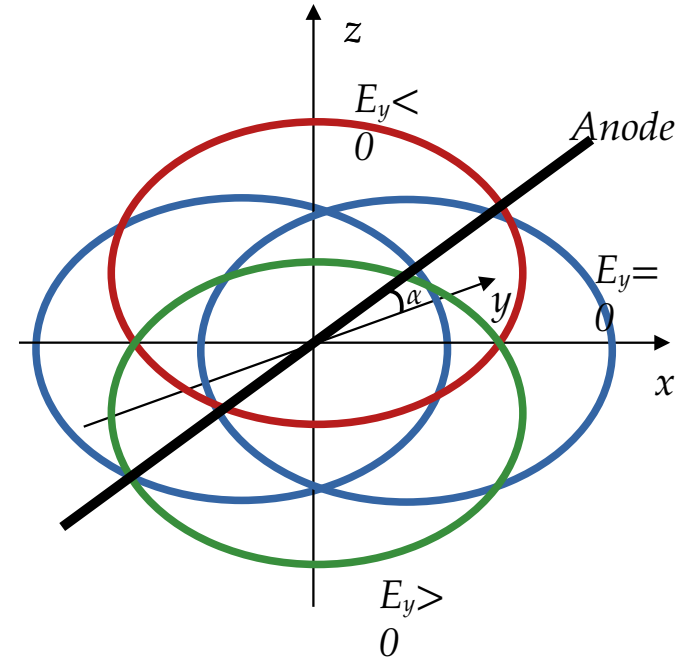
- A non-zero average  $E_y$  field can be generated if the orbit of the muons is elliptical and at the same time it is not perpendicular to the axis of the anode.
  - the average field will be zero if the center of the orbit lies on the  $x$  axis
  - it is positive if it lies on the  $z$  axis above zero and negative if below zero
- In the general case the orbit will be eccentric due to the inward radial Lorentz force from the freeze field





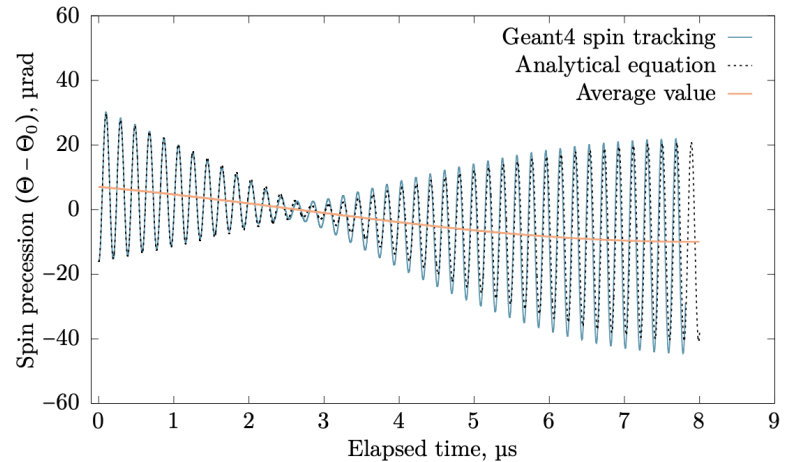
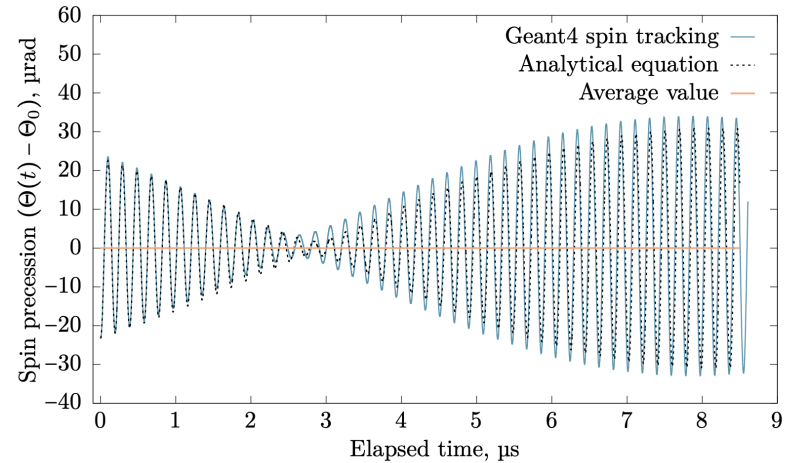
# Non-circular muon orbit

- The effect was observed also in the Geant4 simulations and is consistent with the analytical estimate
- Calculations with the analytical equations show that for  $\alpha = 0.1^\circ$  and orbit displacements up to 5 mm the eccentricity of the orbit should be kept below 0.1
- The eccentricity caused by the freeze field is significantly lower and does not pose a problem
- This effect could constrain the magnetic field uniformity (analysis pending)



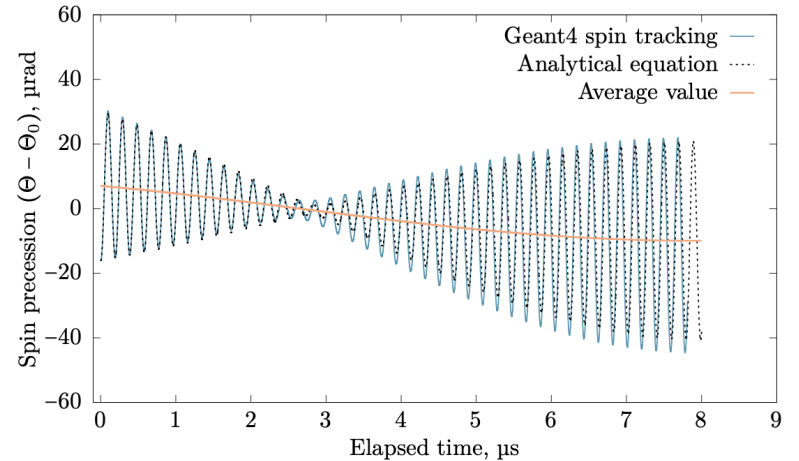
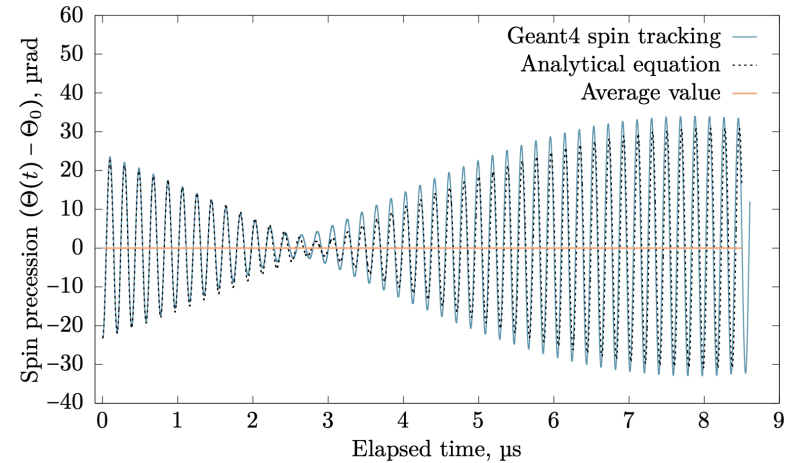
# Comparison with G4

- Compared the analytical equations with a Geant4 simulation with the same parameters (weakly focusing coil current, radius; initial spin vector; etc...)
- In both attempts the frozen spin condition is not perfectly met (for illustration)
- Top:  $E_y = 0$ ; Bottom:  $E_y = E_{freeze}/10^6$ 
  - Note: bottom trend is similar to EDM of  $10^{-21}$  e.cm



# Comparison with G4

- Note that the oscillation frequency is not perfect as the fields are described by first order approximation
- Nevertheless, the equations describe the spin precession well in a very general scenario



# Systematic effects

- The observed change in the asymmetry between the upstream and downstream detectors due to a non-zero EDM is to a first approximation equal to:

$$\dot{A} = \frac{\eta}{2} \frac{e}{m_0} \beta_z B_y \alpha P.$$

- Where  $\eta \sim 10^{-9}$  for  $d_e = 10^{-23} e \cdot \text{cm}$
- It has a similar meaning as the anomalous magnetic moment  $a \sim 10^{-3}$
- One can expect that effects due to the magnetic dipole moment should be suppressed to a level better than  $10^{-6}$

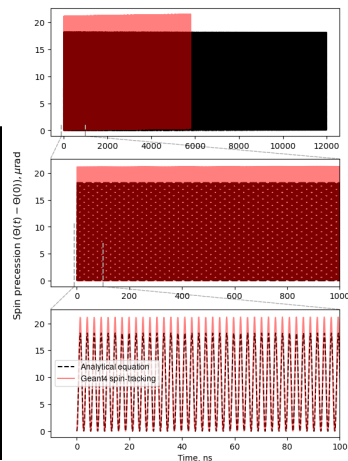
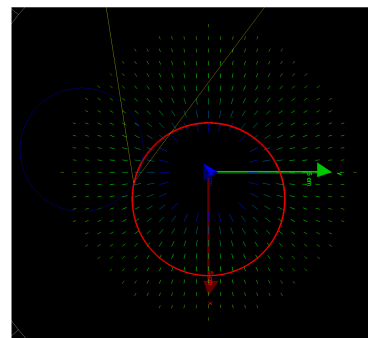
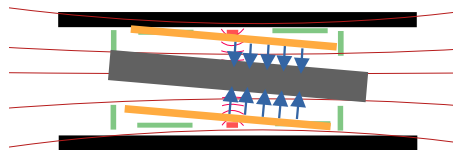
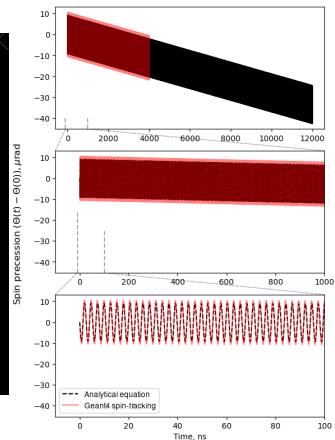
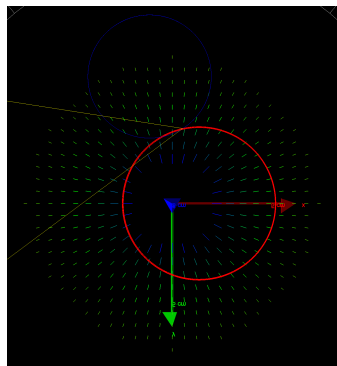
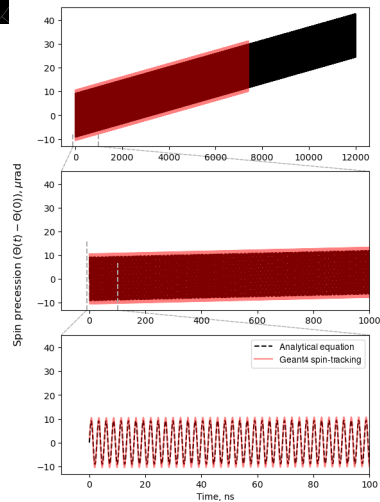
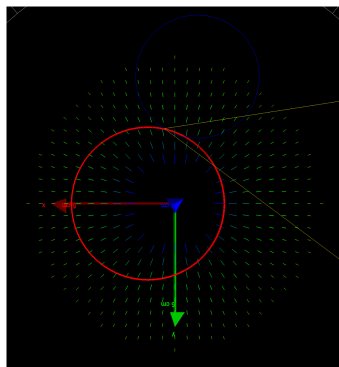
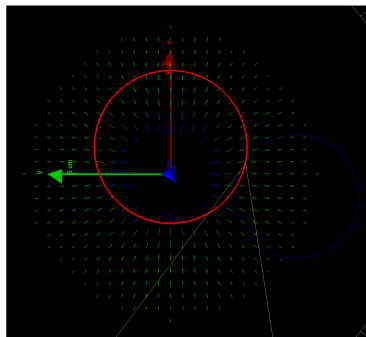
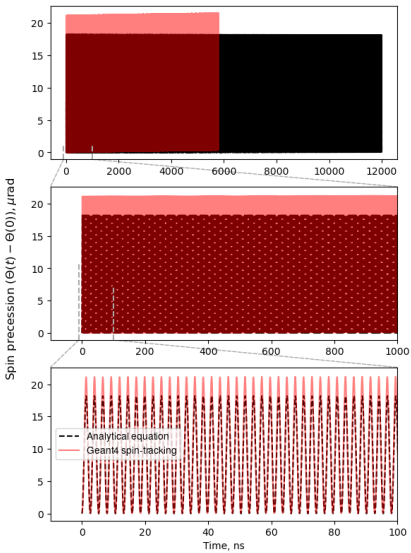
$$\vec{\Omega} = -\frac{e}{m_0} \left[ \underbrace{a\vec{B} + \left( \frac{1}{\gamma^2 - 1} - a \right) \frac{\vec{\beta} \times \vec{E}}{c}}_{\text{MD}} + \underbrace{\frac{\eta}{2} \left( \frac{\vec{E}}{c} + \vec{\beta} \times \vec{B} \right)}_{\text{ED}} \right]$$

MD

ED

M

M



$$\alpha(t; \omega, \beta_0) = -\frac{1}{2\omega} \Omega_x \Omega_y t \sin(\beta_0)$$